ACS APPLIED MATERIALS & INTERFACES

Research Article

www.acsami.org

Composite of Macroporous Carbon with Honeycomb-Like Structure from Mollusc Shell and $NiCo_2O_4$ Nanowires for High-Performance Supercapacitor

Wei Xiong,[†] Yongsheng Gao,[‡] Xu Wu,[†] Xuan Hu,[†] Danni Lan,[†] Yangyang Chen,[†] Xuli Pu,[§] Yan Zeng,[†] Jun Su,[†] and Zhihong Zhu*[,†]

[†]Institute of Nano-Science and Nano-Technology, College of Physical Science and Technology, Central China Normal University, Wuhan 430079, P. R. China

[‡]College of Pharmacy, Hubei University of Chinese Medicine, Huangjia Lake West Road, Wuhan 430065, P. R. China

[§]Xiamen Entry-Exit Inspection and Quarantine Bureau of the People's Republic of China, Xiamen 36102, P. R. China

Supporting Information

ABSTRACT: Novel biological carbon materials with highly ordered microstructure and large pore volume have caused great interest due to their multifunctional properties. Herein, we report the preparation of an interconnected porous carbon material by carbonizing the organic matrix of mollusc shell. The obtained three-dimensional carbon skeleton consists of hexangular and tightly arranged channels, which endow it with efficient electrolyte penetration and fast electron transfer, enable the mollusc shell based macroporous carbon material (MSBPC) to be an excellent conductive scaffold for supercapacitor electrodes. By growing $NiCo_2O_4$ nanowires on the obtained MSBPC, $NiCo_2O_4$/MSBPC composites were synthesized. When used on supercapacitor electrode, it exhibited anomalously high specific capacitance (~1696 F/g), excellent rate performance (with the capacity retention of 58.6% at 15 A/g) and outstanding cycling stability (88% retention after 2000 cycles). Furthermore, an all-solid-state symmetric supercapacitor was also assembled based on this $NiCo_2O_4$/MSBPC electrode and showed good electrochemical performance with an energy density of 8.47 Wh/kg at 1 A/g, good stability over 10000 cycles. And we believe that more potential applications beyond energy storage can be developed based on this MSBPC.

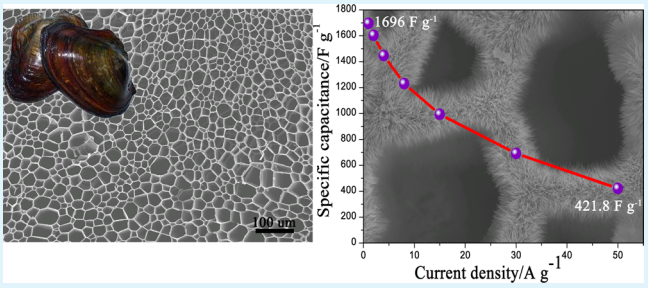

KEYWORDS: *macroporous carbon, honeycomb-like structure, mollusc shell, $NiCo_2O_4$, nanowires, high-performance supercapacitor*

INTRODUCTION

Nowadays, the challenge of fitting more power into greener and tinier spaces to meet the urgent need of environment-friendly and high-efficiency energy sources becomes increasingly considerable.[1,2] As one of the most promising energy storage devices, electrochemical supercapacitors (ESs) have drawn extensive attention due to their excellent characteristics, such as short charging time, high power output, long-term cycling stability, and so forth.[3−6] Such advantages are what the dielectric capacitors or batteries/fuel cells lacked.[7,8] The energy storage properties of the ES are mainly determined by the electrode material,[6] pseudocapacitors, which usually utilize transition metal oxides and conducting polymers as electrode materials always show great advantage on the energy performance due to their storage mechanism of redox processes. However, for transition metal oxides electrode materials, they always suffer from poor electrical/ionic conductivity, which will significantly reduce their electrochemical behavior, especially the power performance.[9,10] So the most important issue in designing these electrode materials is to provide high ways for electron delivery and ion diffusion. One of the feasible ways to solve this problem is incorporation of nanosized metal oxides with carbon based material, using the unique nanostructure and utilizing electrically conductive carbon framework to accelerate the electron transfer and enhance the ion diffusion, to promote the transition metal oxides electrode materials closed to their high theoretical capacity.[10]

Graphene and carbon nanotubes (CNTs) are the widely used carbon substrate with superior energy storage-favorable properties and have sparked extensive exploration in recent years.[11,12] Although with large surface area, great flexibility, or good mechanical properties, these carbon-based backbones still exhibit unsatisfactory parts due to insuperable restacking or aggregation problem,[2,13−15] which disenable them to form highly ordered structures, will critically affect their phys-

Received: August 16, 2014
Accepted: October 21, 2014
Published: October 21, 2014

icochemical properties, especially serving as the supporting substrate which good electrolyte penetration and ion diffusion are needed. Furthermore, prohibitive price and tedious fabrication processes are also important factors that hinder the practical application of graphene/CNT based carbon substrates. So, synthesis of facile and low-cost carbon materials with delicate structures derived from biotemplate has become a research hotspot in recent years.[16−20]

The reason why biobased carbon attracts wide interesting is that natural highly ordered structures with excellent physicochemical properties can be easily obtained from them without complicated chemical/physical processes.[21] For instance, Liu et al. synthesized the highly ordered carbon nanofiber arrays using crab shell as a hard-template and exhibited excellent specific capacitance of 152 F/g.[21] Qian et al. synthesized heteroatom doped porous carbon flakes via carbonization of human hair and showed high specific capacitance of 340 F/g at 1 A/g.[22] These works all demonstrated the specific advantages of biotemplate derived carbon materials in preparing high-performance electrode materials.[23] So, by virtue of the unique natural structure of biotemplate derived highly conductive carbon material and the high theoretical capacity of transition metal oxides to get the high performance supercapacitor electrode materials will be definitely a fantastic way to develop the pseudocapacitors.

In this work, for the first time, we found another kind of novel honeycomb-like biocarbon substrate, mollusc shell based macroporous carbon material (MSBPC), which showed a highly ordered and interconnected structure consisted of a dense net of well-aligned hexagonal channel arrays. The MSBPC was obtained from mollusc shells simply through acid treatment and carbonization, since the shells mainly consist of calcium carbonate crystal and biomacro-molecules. Particularly, the preparation of the MSBPC can be very cheap and renewable. This would be of great benefit to their widespread commercialization. Honeycomb-like structure possesses the most geometric efficiency, which means use the least amount of material to create the maximum and most solid spaces. The channel arrays are very uniform, when used on supercapacitor electrode materials, will make the whole surface, including the inner walls, of the channel can be served as the substrate to loading active materials, and at the same time, the electrolyte can be very easy to infiltrate into the surface of the loaded active material and can effectively increase the ion diffusion rate of the electrode. On the other hand, these channel arrays are interconnected, which is very good for the fast electron transfer throughout the whole electrode. Then, to validate its potential application on the energy storage, we directly grow spinel nickel cobaltite ($NiCo_2O_4$) nanowires on this MSBPC. The $NiCo_2O_4$ always possesses better electrochemical activity than single components of nickel oxide and cobalt oxide since the $NiCo_2O_4$ combines contributions from both nickel and cobalt ions.[24] As a result, the obtained novel $NiCo_2O_4$/MSBPC composites showed an excellent electrochemical performance, and an all-solid-state symmetric supercapacitor was also assembled based on this $NiCo_2O_4$/MSBPC electrode. The prepared all-solid-state supercapacitor exhibited a specific capacitance of 61 F/g at a current density of 1 A/g, 85% of the capacitance could still be maintained after 10000 cycles at a high current of 400 mA and can light a LED. This obviously suggests that the MSBPC can be potentially used in supercapacitors.

RESULTS AND DISCUSSION

The fabrication process of the $NiCo_2O_4$/MSBPC composites is shown in Scheme 1. First, MSBPC was obtained by using the mollusc shell as templates and then grew the $NiCo_2O_4$ nanowires on it through a simple hydrothermal method. As shown in Figure 1a, a macroporous carbon network was prepared via carbonization of mollusc shell, where large scale continuous channel without any collapse and fracture can be obviously observed. The size of the pore is relatively uniform and can be estimated to around 20 um. Hexagonal channel structure can be observed clearly (Figure 1b). It is worth mentioning that even within the same biology, the morphology and size of the pore may not be the same (Supporting Information Figure S1a and b). The corresponding XRD pattern is shown in Supporting Information Figure S1c, a broad peak around 25° of 2 theta, indicating the typical XRD pattern for the amorphous carbon.[25] The BET surface areas and pore size distribution of MSBPC were also investigated by N_2 adsorption−desorption measurements (Supporting Information Figure S2a and b). The Supporting Information Figure S2a shows a steep type-I isotherm with an obvious hysteresis loop, indicating the coexistence of micropores and mesopores structures formed in MSBPC. From Supporting Information Figure S2b, we can find there are few pores larger than 10 nm and the average diameter of pore is 1.98 nm. The BET surface area of the MSBPC is around 440.36 m^2g^{-1}.

This unique interconnected 3D network structure suggests that the MSBPC have potential applications as substrate for the synthesis of 3D functional composite materials.

Scheme 1. Preparation Process of $NiCo_2O_4$/MSBPC Composites

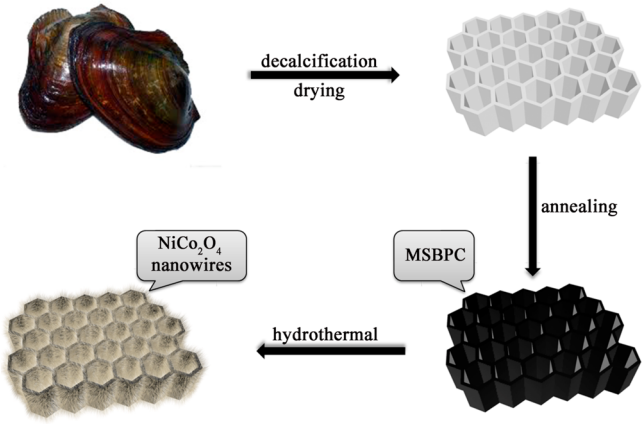

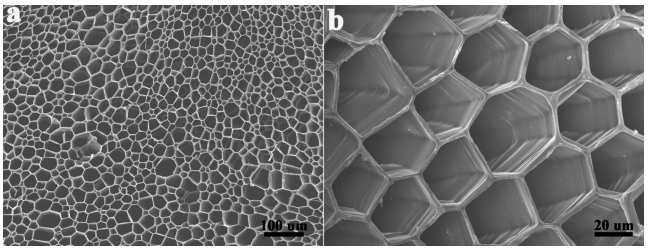

Figure 1. (a) SEM image of the MSBPC. (b) Magnified SEM image of the MSBPC.

Under the guidance of this idea, the $NiCo_2O_4$/MSBPC composites were successfully synthesized by a facile greener hydrothermal method. Figure 2a and b show the microstructure

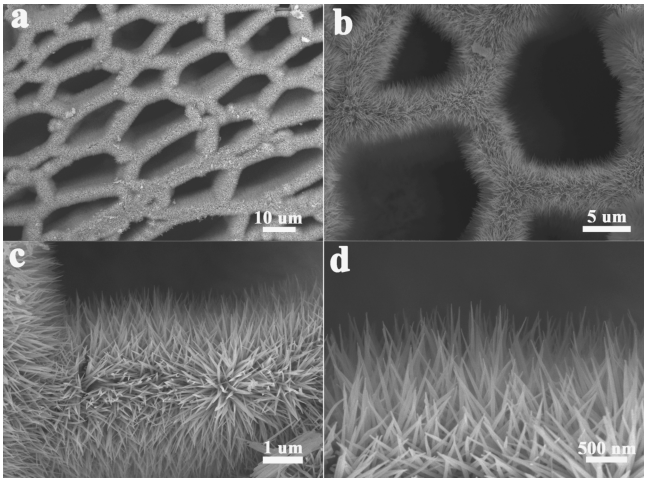

Figure 2. (a, b) SEM images of the $NiCo_2O_4$/MSBPC composites. (c, d) High-magnification SEM images of the $NiCo_2O_4$ nanowires.

and morphology of the $NiCo_2O_4$ nanowires on MSBPC. It demonstrates that the $NiCo_2O_4$ are uniformly grown on the MSBPC and the interconnected porous skeleton of the MSBPC can be retained without any collapse. It can also be found that the inner wall of channel is fully and uniformly covered by $NiCo_2O_4$ nanowires with an average length around 1.5 μm (Supporting Information Figure S3a and Figure 3b), which increases the width of the carbon skeleton and further improves space utilization of the MSBPC. Figure 2c and d show the higher magnification scanning electron microscopy (SEM) images of the product, which indicates that $NiCo_2O_4$ nanowires with high density are grown vertically on MSBPC, forming a high aligned nanowires arrays. The final composites still keep the orderly structure and offer large surface area for Faradaic reactions. Meanwhile the MSBPC is served as conducting substrate and the $NiCo_2O_4$ directly grows on it as binder-free electrodes, this kind of connection provides short and straight electron pathways, which can allow efficient electron transport in the electrode.[24,26−28]

The X-ray diffraction (XRD) analysis confirmed the formation of the $NiCo_2O_4$ phase and the XRD pattern in Figure 3a (A) coincides with $NiCo_2O_4$/MSBPC precisely. In detail, the diffraction peaks at 18.96, 31.26, 36.26, 44.19, 59.35, 65.23, and 76.70° can be indexed as the (111), (220), (311), (400), (511), (440), and (622) crystal planes of $NiCo_2O_4$. All the reflection peaks can be easily indexed to the $NiCo_2O_4$, a broad peak at 2θ = 25°, indicating that the substrate is amorphous carbons (MSBPC), manifesting that the $NiCo_2O_4$ nanowires have been successfully fabricated on the surface of MSBPC substrate. The sharp diffraction in Figure 3a (B) shows the good crystallinity of pure $NiCo_2O_4$, and no peaks from other crystallized phases are observed, indicating the formation of pure $NiCo_2O_4$ product.[26,29]

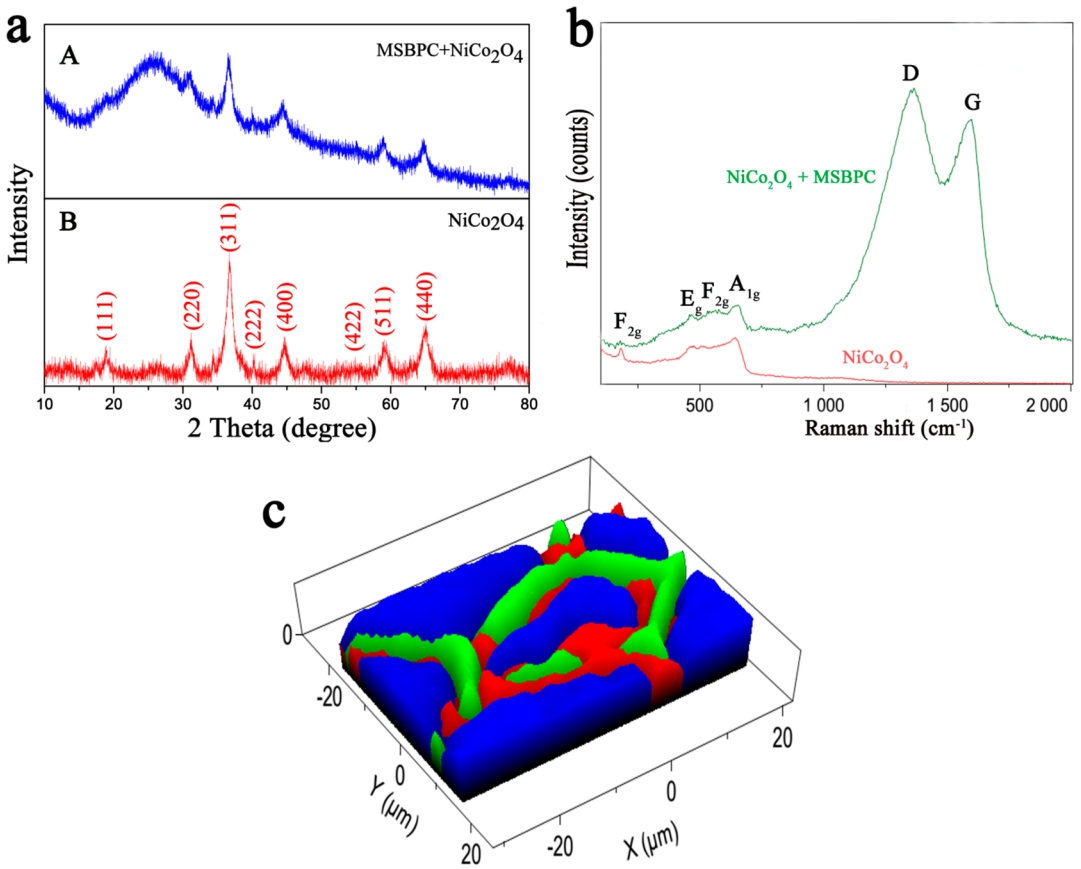

Figure 3. (a) XRD patterns of (A) $NiCo_2O_4$/MSBPC composites, (B) pure $NiCo_2O_4$. (b) Raman spectra and (c) Raman image of the$NiCo_2O_4$/MSBPC composites.

Figure 3b further reveals the Raman spectrum of pure $NiCo_2O_4$ and $NiCo_2O_4$/MSBPC composites in the range from 0 to 2000 cm^{-1}. The Raman spectrum of the MSBPC exhibits vibrational peaks around 1347 and 1585 cm^{-1}, which can be contributed to the D and G bands.[30] Additional peaks below a wavenumber of 700 cm^{-1} (the peaks at 186, 456, 506, and 649 cm^{-1} correspond to F_{2g}, E_g, F_{2g}, and A_{1g} modes of the $NiCo_2O_4$ nanowires, respectively.[31]) are also obtained and can be assigned to vibrational modes of the $NiCo_2O_4$. Raman spectrum mapping characterization of the $NiCo_2O_4$ /MSBPC composites is shown in Figure 3c. From the simulation diagram, we can directly observe the structure of MSBPC and the cover-rate of $NiCo_2O_4$ (the red color represents $NiCo_2O_4$, the green color represents MSBPC, the blue color represents hole). Interestingly, the appearance of MSBPC substrate in the mapping further suggests that $NiCo_2O_4$ nanowires have been successfully fabricated on the MSBPC. However, most of the final product, the carbon skeleton is almost completely covered (Supporting Information Figure S4).

To further characterize the morphological and structural features of the $NiCo_2O_4$/MSBPC composites, transmission electron microscopy (TEM), high resolution TEM (HRTEM), and selected area electron diffraction (SAED) studies were performed. The $NiCo_2O_4$ nanowires are 50 nm in diameter, and it gradually decreases to only several nanometers at the tips (Figure 4a), and its mesoporous structure is also confirmed by

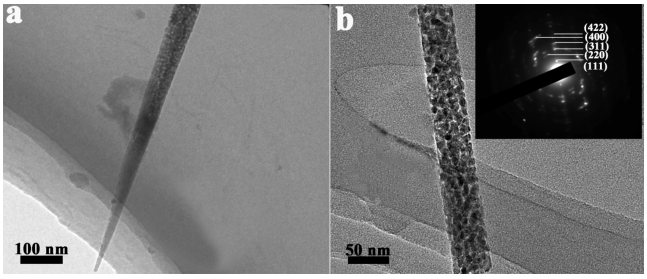

Figure 4. (a) TEM image and (b) HRTEM image, the inset shows the SAED pattern of the $NiCo_2O_4$.

TEM image (Figure 4b), with the sizes of these pores estimated to several nanometers, which will increases the amount of electroactive sites and facilitates the electrolyte penetration. The well-defined diffraction rings in the SAED pattern (inset in Figure 4b) indicates the polycrystalline nature of the $NiCo_2O_4$ nanowires.

The electrochemical properties of the $NiCo_2O_4$/MSBPC composites were investigated by using a three-electrode mode in a 2 M KOH solution. Figure 5a shows the typical cyclic voltammetry (CV) curves of the $NiCo_2O_4$/MSBPC composites with various sweep rates ranging from 10 to 40 mV s^{-1} in the potential range 0−0.55 V. The shape of the CV curves is much in line with previous reports on $NiCo_2O_4$ in KOH solution.[6,10,24,31−33] Clearly, a distinct pair of redox peaks is visible in different scan rates, which surely confirms the pseudocapacitive behavior of the $NiCo_2O_4$. The redox peaks can be attributed to the reaction of M−O/M−O−O−OH (M represents Ni and Co ions) associated with OH^- anions.[9,10,32] With the increase of the scanning rate, the position of the anodic peak shifts from 0.35 to 0.42 V, which mainly due to the charge transfer kinetics is the limiting step of the reaction.[26,34,35] In order to exclude the effect of nickel foam, we also present the CV curve of the nick foam at 10 mV s^{-1} (Figure 5c). The result shows the signal of nickel foam is quite weak, suggesting that the capacitive contribution from the nickel foam is negligible.[36] Figure 5c also compares the CV curves of the $NiCo_2O_4$/MSBPC composites and pure $NiCo_2O_4$. The CV integrated area of the $NiCo_2O_4$/MSBPC composites is much larger than the pure $NiCo_2O_4$, which suggest the specific capacitance is remarkably improved than pure $NiCo_2O_4$. Figure 5d further displays the comparison of galvanostatic charge−discharge (GCD) curves for pure $NiCo_2O_4$ and $NiCo_2O_4$/MSBPC composites at the same current density of 1 A/g, the charge−discharge time of pure $NiCo_2O_4$ is obviously shorter than $NiCo_2O_4$/MSBPC composites. This suggests that the MSBPC plays a key role in the promotion of the electrochemical properties.

To further evaluate the electrochemical performance of the $NiCo_2O_4$/MSBPC composites for practical application, the GCD tests were conducted at various current densities ranging from 1 to 15 A/g. As shown in Figure 5b. To obtain the accurate values of specific capacitance for nonlinear GCD plot resulted from a quasi-reversible faradic reaction, we calculate it based on the following equation:

$$c = \frac{2i_m \int V \mathrm{d}t}{V^2|_{v_i}^{v_f}} \quad (1)$$

Where $i_m = I/m$ (A g^{-1}) represents the current density, I is the constant discharge current and m denotes the weight of active electrode. $\int V\mathrm{d}t$ refers to the integral current area of the discharge curve, where V refers to the potential with initial and final values of the V_i and V_F, respectively.[37,38] The difference between the nonlinear and linear GCD plot in algorithms is provided in the Supporting Information Figure S6.

The $NiCo_2O_4$/MSBPC composites exhibited a high specific capacitance of 1696 F/g at a current density of 1 A/g and good rate performance (Figure 6a), 1604 F/g at 2 A/g, 1447.5 F/g at 4 A/g, 1231 F/g at 8 A/g, 993.7 F/g at 15 A/g, 691.8 F/g at 30 A/g. Even the current density increases to 50 A/g, the specific capacitance is still as high as 421.8 F/g. This high specific capacitance with such an excellent rate-capability has rarely been reported previously.[5,14,35] The excellent electrochemical performance of the $NiCo_2O_4$/MSBPC composites can be attributed to their unique structural feature. First, due to interconnected network of the MSBPC, the electronic can quickly spread throughout the network. Meanwhile, binder-free electrodes provide reliable electrical connection to the $NiCo_2O_4$ to accelerate the electron transport. Second, large channel volume ensures the efficient protons penetration and high surface area of the inner wall supports $NiCo_2O_4$ nanowires array can be great beneficial for the effective utilization of active materials. So, manufacturing this unique macroporous carbon network as substrates not only improves the electrical conductivity of $NiCo_2O_4$ but also facilitates the rapid transport of the ions in the electrolyte. Third, the uniformly aligned mesoporous $NiCo_2O_4$ nanowires array offers large surface area, allowing facile electrolyte access for fast redox reaction.

The long-term cycling performance is a critical requirement for supercapacitor devices. Cycling stability of the $NiCo_2O_4$/MSBPC composites and the pure $NiCo_2O_4$ was conducted using GCD cycles at 5 A/g, as shown in Figure 6b. The specific capacitance of $NiCo_2O_4$/MSBPC composites increased in the first 250 cycles, which can be attributed to the complete activation of the electrode. Then, it gradually stabilized at 1100 F/g over 2000 cycles, resulting in an overall capacitance loss of

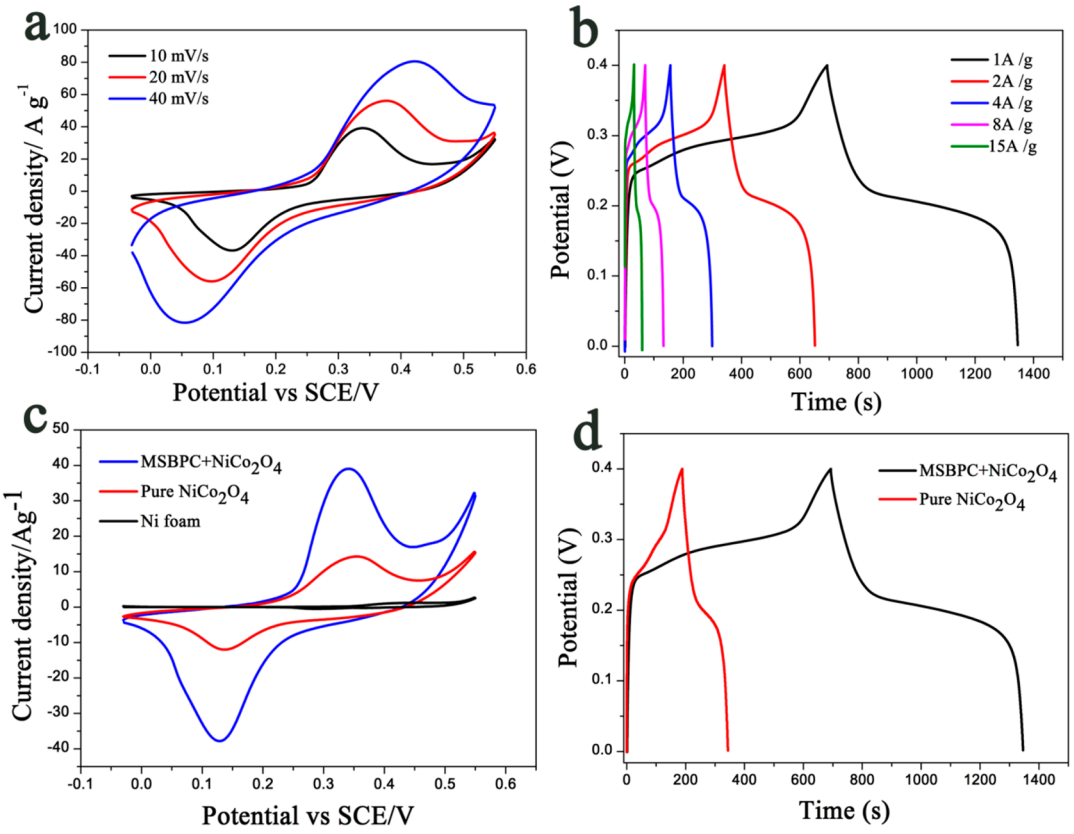

Figure 5. (a) CV curves at various scan rates ranging from 10 to 40 mV s^{-1}. (b) Charge−discharge curves at different current densities. (c) CV curves of MSBPC/$NiCo_2O_4$ composites, pure $NiCo_2O_4$, and nickel foam at 10 mV s^{-1}. (d) Galvanostatic charge−discharge at a current density of 1 A g^{-1} for the MSBPC/$NiCo_2O_4$ composites and pure $NiCo_2O_4$.

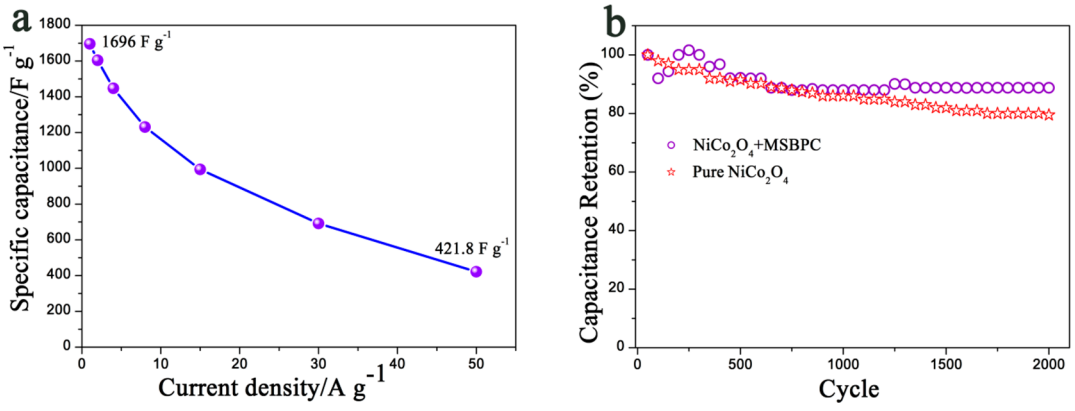

Figure 6. (a) Specific capacitance versus different charge−discharge current density plots. (b) Cycling performance of $NiCo_2O_4$/MSBPC composites and pure $NiCo_2O_4$ at 5 A/g.

only 12%. This cycling stability is superior to the pure $NiCo_2O_4$, in which the capacitance decreases by 21% after 2000 cycles. Such excellent cycle stability is mainly due to the interconnected MSBPC reinforce the electrode structure to inhibit the structure collapse of $NiCo_2O_4$ nanowires during cycling.

In order to evaluate the potential of $NiCo_2O_4$/MSBPC based supercapacitor as energy storage, an all-solid-state symmetric supercapacitor was designed by using nickel foam as current collector, the poly(vinyl alcohol)/KOH as separator and electrolyte, $NiCo_2O_4$/MSBPC as electrode. Figure 7a schematically shows the procedures for preparing the symmetric supercapacitor. Figure 7b presents the typical CV curves of the symmetric supercapacitor at the scan rates of 10, 20, 40 mV/s; the shapes of the CV curves suggest an ideal capacitive behavior, from which we can find the area of CV curves increases obviously with the increasing of the scan rate, indicating the rapid diffusion of the ions in polymer electrolyte. Moreover, solid-state capacitor delivered a much higher working voltage range (from 0 to 1 V) than a three-electrode cell (from 0 to 0.55 V), which will facilitate a more practical application of supercapacitors.

The GCD curves at various current densities from 1 to 8 A/g are demonstrated in Figure 7c, the shapes of the GCD curves tend toward triangular-shaped and the discharging time is almost equal to the charging time, suggesting the excellent

dx.doi.org/10.1021/am5055228 | ACS Appl. Mater. Interfaces 2014, 6, 19416−19423

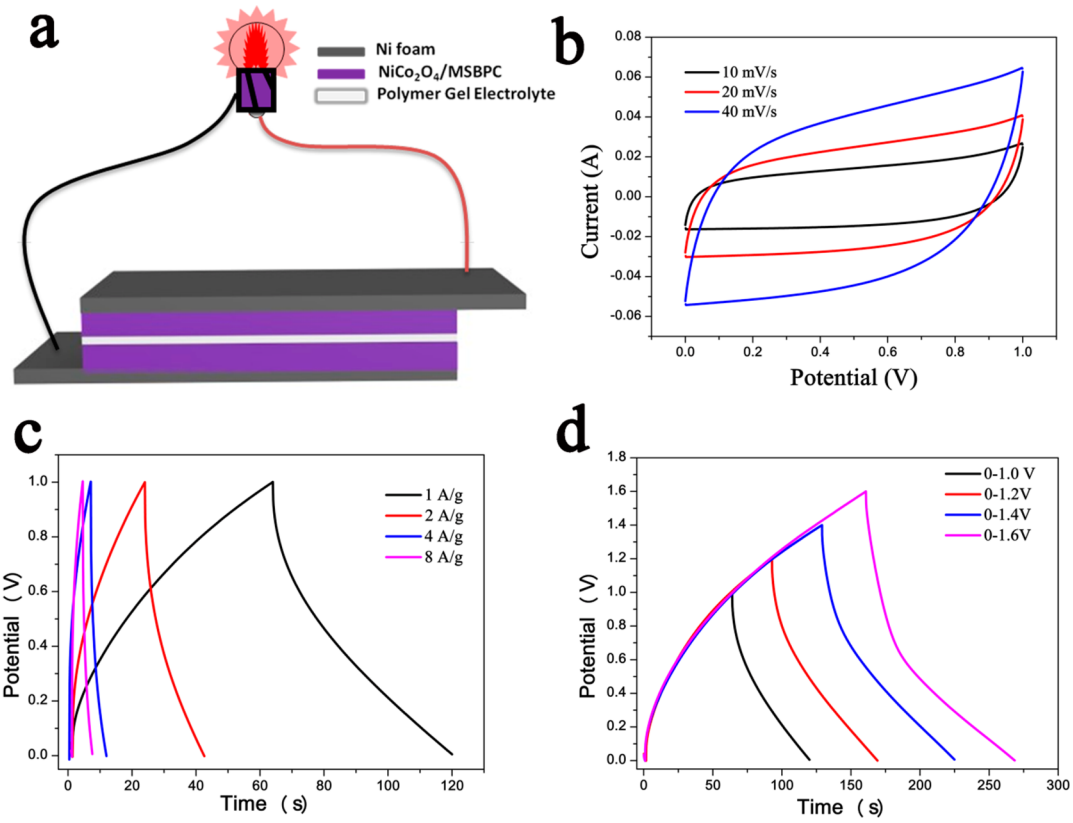

Figure 7. (a) Schematic diagram of all-solid-state capacitor based on MSBPC/$NiCo_2O_4$ composites. (b) CV curves of solid-state capacitor with different scan rates. (c) GCD curves measured at different current densities of 1, 2, 4, 8 A/g. (d) GCD curves of the SC device collected at different potential windows at current density of 1 A/g.

Coulombic efficiency of our device. The volume capacitance of the symmetric supercapacitor could be calculated by eq 1. The highest capacitance was 60 F/g at 1 A/g and remained at 24.7 F/g at 8 A/g, demonstrating an excellent rate capability.

Higher voltage range will lead to greater energy density.[33,39] To evaluate the potential window of the $NiCo_2O_4$/MSBPC based supercapacitor, the GCD curves at 1 A/g with different potential widows was measured (Figure 7d). Owing to a relatively low resistance of the $NiCo_2O_4$/MSBPC electrode, it still showed good reversibility and electrochemical stability, when the operating voltage rose up to 1.6 V. To demonstrate its practical applications, a red LED (the operating voltage is 1.5−1.8 V) was lighted up by only one piece of SC (Figure 8 inset), illustrating its superior performance. Long cycle life stability is another critical requirement for practical applications. As shown in Figure 8, excellent stability was obtained between 0 and 1 V at high current (400 mA), remained 85% during the entire cycling after 10000 charge−discharge cycles. Such superior cycle stability is attributed to the role of the PVA as the binder, and the polymer electrolyte can protect the structure of $NiCo_2O_4$/MSBPC based electrode. Besides, this kind of all-solid-state symmetric supercapacitor not only has a simple assembly processes but also avoids the risk of electrolyte leakage for liquid electrolyte capacitors.

From the results mentioned above, we conclude that the $NiCo_2O_4$/MSBPC based supercapacitor is promising in practical applications. As a kind of novel conductive backbone, the MSBPC is highly effective for improving the electrochemical performance of supercapacitor. Additionally, this honeycomb-like structure provides an inspiration to synthesis

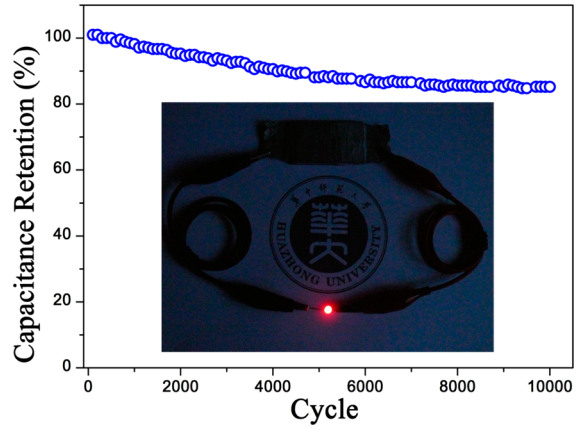

Figure 8. Cycling performances during 10000 cycles at a high current 400 mA. Inset: a red LED powered by SC device.

the other carbon-based composite materials for application in energy storage or other emerging research fields.

CONCLUSIONS

In summary, a novel macroporous carbon material of MSBPC has been obtained from mollusc shell via a simple decalcification and annealing process and was first used in electrochemical energy storage. When combined with $NiCo_2O_4$, exhibited high specific capacitances, excellent rate capability, and good cycle stability. A high specific capacitance of 1696 F/g was achieved at a current density of 1 A/g (even 421.8 F/g at 50 A/g) and only 12% capacitance loss after 2000

cycles at 5 A/g based on the obtained $NiCo_2O_4$/MSBPC composites. Furthermore, an all-solid-state supercapacitor with excellent electrochemical performances was also successfully fabricated and of great relevance to applications. We believe that this bioinspired carbon material can be further utilized to combine with other metal oxides or conductive polymers, and its excellent structure and conductivity might offer great promise for fabrication of high-performance energy storage devices; more potential applications beyond energy storage such as biosensors and catalysis can even be developed based on this MSBPC.

■ ASSOCIATED CONTENT

Supporting Information

Experimental details and additional supporting data such as SEM images, XRD pattern, and Raman spectrum mapping. This material is available free of charge via the Internet at http://pubs.acs.org.

■ AUTHOR INFORMATION

Corresponding Author

*E-mail: zhzhu@phy.ccnu.edu.cn.

Author Contributions

W.X. and Y. G. contributed equally to this work.

Notes

The authors declare no competing financial interest.

■ ACKNOWLEDGMENTS

This work was financially supported by self-determined research funds of CCNU from the colleges' basic research and operation of MOE (No.CCNU13A05007), the Key Scientific Project of Wuhan City (No.2013011801010598), the Scientific Project of AQSIQ (No.2013IK093) and the National Natural Science Foundation of China (No. 50802032).

■ REFERENCES

(1) Wu, X.; Zeng, Y.; Gao, H.; Su, J.; Liu, J.; Zhu, Z. Template Synthesis of Hollow Fusiform $RuO_2{\cdot}xH_2O$ Nanostructure and Its Supercapacitor Performance. *J. Mater. Chem. A* **2013**, *1*, 469−472.

(2) Liu, S.; Sun, S.; You, X.-Z. Inorganic Nanostructured Materials for High Performance Electrochemical Supercapacitors. *Nanoscale* **2014**, *6*, 2037−2045.

(3) Tang, P.; Han, L.; Zhang, L. Facile Synthesis of Graphite/PEDOT/MnO_2 Composites on Commercial Supercapacitor Separator Membranes as Flexible and High-Performance Supercapacitor Electrodes. *ACS Appl. Mater. Interfaces* **2014**, *6*, 10506−10515.

(4) Lan, D.; Chen, Y.; Chen, P.; Chen, X.; Wu, X.; Pu, X.; Zeng, Y.; Zhu, Z. Mesoporous CoO Nanocubes@Continuous 3D Porous Carbon Skeleton of Rose Based Electrode for High-Performance Supercapacitor. *ACS Appl. Mater. Interfaces* **2014**, *6*, 11839−11845.

(5) Butt, F. K.; Tahir, M.; Cao, C.; Idrees, F.; Ahmed, R.; Khan, W. S.; Ali, Z.; Mahmood, N.; Tanveer, M.; Mahmood, A. Synthesis of Novel ZnV_2O_4 Hierarchical Nanospheres and Their Applications as Electrochemical Supercapacitor and Hydrogen Storage Material. *ACS Appl. Mater. Interfaces* **2014**, *6*, 13635−13641.

(6) Jiang, H.; Ma, J.; Li, C. Hierarchical Porous $NiCo_2O_4$ Nanowires for High-Rate Supercapacitors. *Chem. Commun.* **2012**, *48*, 4465−4467.

(7) Rakhi, R. B.; Chen, W.; Hedhili, M.; Cha, D.; Alshareef, H. N. Enhanced Rate Performance of Mesoporous Co_3O_4 Nanosheet Supercapacitor Electrodes by Hydrous RuO_2 Nanoparticle Decoration. *ACS Appl. Mater. Interfaces* **2014**, *6*, 4196−4206.

(8) Kim, M.; Kim, J. Redox Deposition of Birnessite-Type Manganese Oxide on Silicon Carbide Microspheres for Use as Supercapacitor Electrodes. *ACS Appl. Mater. Interfaces* **2014**, *6*, 9036−9045.

(9) Zhang, G. Q.; Wu, H. B.; Hoster, H. E.; Chan-Park, M. B.; Lou, X. W. D. Single-Crystalline $NiCo_2O_4$ Nanoneedle Arrays Grown on Conductive Substrates as Binder-Free Electrodes for High-Performance Supercapacitors. *Energy Environ. Sci.* **2012**, *5*, 9453−9456.

(10) Huang, L.; Chen, D.; Ding, Y.; Feng, S.; Wang, Z. L.; Liu, M. Nickel−Cobalt Hydroxide Nanosheets Coated on $NiCo_2O_4$ Nanowires Grown on Carbon Fiber Paper for High-Performance Pseudocapacitors. *Nano Lett.* **2013**, *13*, 3135−3139.

(11) Wang, H.; Holt, C. M.; Li, Z.; Tan, X.; Amirkhiz, B. S.; Xu, Z.; Olsen, B. C.; Stephenson, T.; Mitlin, D. Graphene-Nickel Cobaltite Nanocomposite Asymmetrical Supercapacitor with Commercial Level Mass Loading. *Nano Res.* **2012**, *5*, 605−617.

(12) Zhu, G.; He, Z.; Chen, J.; Zhao, J.; Feng, X.; Ma, Y.; Fan, Q.; Wang, L.; Huang, W. Highly Conductive Three-Dimensional MnO_2−Carbon Nanotube−Graphene−Ni Hybrid Foam as a Binder-Free Supercapacitor Electrode. *Nanoscale* **2014**, *6*, 1079−1085.

(13) Lota, G.; Fic, K.; Frackowiak, E. Carbon Nanotubes and Their Composites in Electrochemical Applications. *Energy Environ. Sci.* **2011**, *4*, 1592−1605.

(14) Wang, H.-W.; Hu, Z.-A.; Chang, Y.-Q.; Chen, Y.-L.; Wu, H.-Y.; Zhang, Z.-Y.; Yang, Y.-Y. Design and Synthesis of $NiCo_2O_4$−Reduced Graphene Oxide Composites for High Performance Supercapacitors. *J. Mater. Chem.* **2011**, *21*, 10504−10511.

(15) El-Kady, M. F.; Strong, V.; Dubin, S.; Kaner, R. B. Laser Scribing of High-Performance and Flexible Graphene-Based Electrochemical Capacitors. *Science* **2012**, *335*, 1326−1330.

(16) Wu, X.-L.; Wen, T.; Guo, H.-L.; Yang, S.; Wang, X.; Xu, A.-W. Biomass-Derived Sponge-Like Carbonaceous Hydrogels and Aerogels for Supercapacitors. *ACS Nano* **2013**, *7*, 3589−3597.

(17) Saha, D.; Li, Y.; Bi, Z.; Chen, J.; Keum, J. K.; Hensley, D. K.; Grappe, H. A.; Meyer, H. M., III; Dai, S.; Paranthaman, M. P. Studies on Supercapacitor Electrode Material from Activated Lignin-Derived Mesoporous Carbon. *Langmuir* **2014**, *30*, 900−910.

(18) Chen, W.; Zhang, H.; Huang, Y.; Wang, W. A Fish Scale Based Hierarchical Lamellar Porous Carbon Material Obtained Using a Natural Template for High Performance Electrochemical Capacitors. *J. Mater. Chem.* **2010**, *20*, 4773−4775.

(19) Liang, Y.; Wu, D.; Fu, R. Carbon Microfibers with Hierarchical Porous Structure from Electrospun Fiber-Like Natural Biopolymer. *Sci. Rep.* **2013**, *3*, 2045−2322.

(20) Wang, H.; Xu, Z.; Kohandehghan, A.; Li, Z.; Cui, K.; Tan, X.; Stephenson, T. J.; King'ondu, C. K.; Holt, C. M.; Olsen, B. C. Interconnected Carbon Nanosheets Derived from Hemp for Ultrafast Supercapacitors with High Energy. *ACS Nano* **2013**, *7*, 5131−5141.

(21) Liu, H.-J.; Wang, X.-M.; Cui, W.-J.; Dou, Y.-Q.; Zhao, D.-Y.; Xia, Y.-Y. Highly Ordered Mesoporous Carbon Nanofiber Arrays from a Crab Shell Biological Template and Its Application in Supercapacitors and Fuel Cells. *J. Mater. Chem.* **2010**, *20*, 4223−4230.

(22) Qian, W.; Sun, F.; Xu, Y.; Qiu, L.; Liu, C.; Wang, S.; Yan, F. Human Hair-Derived Carbon Flakes for Electrochemical Supercapacitors. *Energy Environ. Sci.* **2014**, *7*, 379−386.

(23) Simon, P.; Gogotsi, Y.; Dunn, B. Where Do Batteries End and Supercapacitors Begin? *Sci. Mag.* **2014**, *343*, 1210−1211.

(24) Zhang, G.; Lou, X. W. D. General Solution Growth of Mesoporous $NiCo_2O_4$ Nanosheets on Various Conductive Substrates as High−Performance Electrodes for Supercapacitors. *Adv. Mater.* **2013**, *25*, 976−979.

(25) Pérez, C. R.; Yeon, S. H.; Ségalini, J.; Presser, V.; Taberna, P. L.; Simon, P.; Gogotsi, Y. Structure and Electrochemical Performance of Carbide−Derived Carbon Nanopowders. *Adv. Funct. Mater.* **2013**, *23*, 1081−1089.

(26) Wang, Q.; Liu, B.; Wang, X.; Ran, S.; Wang, L.; Chen, D.; Shen, G. Morphology Evolution of Urchin-Like $NiCo_2O_4$ Nanostructures and Their Applications as Psuedocapacitors and Photoelectrochemical Cells. *J. Mater. Chem.* **2012**, *22*, 21647−21653.

(27) Wang, H.; Wang, X. Growing Nickel Cobaltite Nanowires and Nanosheets on Carbon Cloth with Different Pseudocapacitive Performance. *ACS Appl. Mater. Interfaces* **2013**, *5*, 6255−6260.
(28) Du, J.; Zhou, G.; Zhang, H.; Cheng, C.; Ma, J.; Wei, W.; Chen, L.; Wang, T. Ultrathin Porous $NiCo_2O_4$ Nanosheet Arrays on Flexible Carbon Fabric for High-Performance Supercapacitors. *ACS Appl. Mater. Interfaces* **2013**, *5*, 7405−7409.
(29) Liu, X.; Zhang, Y.; Xia, X.; Shi, S.; Lu, Y.; Wang, X.; Gu, C.; Tu, J. Self-Assembled Porous $NiCo_2O_4$ Hetero-Structure Array for Electrochemical Capacitor. *J. Power Sources* **2013**, *239*, 157−163.
(30) Kuila, T.; Bose, S.; Mishra, A. K.; Khanra, P.; Kim, N. H.; Lee, J. H. Chemical Functionalization of Graphene and Its Applications. *Prog. Mater. Sci.* **2012**, *57*, 1061−1105.
(31) Deng, F.; Yu, L.; Cheng, G.; Lin, T.; Sun, M.; Ye, F.; Li, Y. Synthesis of Ultrathin Mesoporous $NiCo_2O_4$ Nanosheets on Carbon Fiber Paper as Integrated High-Performance Electrodes for Supercapacitors. *J. Power Sources* **2014**, *251*, 202−207.
(32) He, G.; Wang, L.; Chen, H.; Sun, X.; Wang, X. Preparation and Performance of $NiCo_2O_4$ Nanowires-Loaded Graphene as Supercapacitor Material. *Mater. Lett.* **2013**, *98*, 164−167.
(33) Lu, X.-F.; Wu, D.-J.; Li, R.-Z.; Li, Q.; Ye, S.-H.; Tong, Y.-X.; Li, G.-R. Hierarchical $NiCo_2O_4$ Nanosheets@ Hollow Microrod Arrays for High-Performance Asymmetric Supercapacitors. *J. Mater. Chem. A* **2014**, *2*, 4706−4713.
(34) Wu, Y. Q.; Chen, X. Y.; Ji, P. T.; Zhou, Q. Q. Sol−Gel Approach for Controllable Synthesis and Electrochemical Properties of $NiCo_2O_4$ Crystals as Electrode Materials for Application in Supercapacitors. *Electrochim. Acta* **2011**, *56*, 7517−7522.
(35) Chen, H.; Jiang, J.; Zhang, L.; Qi, T.; Xia, D.; Wan, H. Facilely Synthesized Porous $NiCo_2O_4$ Flowerlike Nanostructure for High-Rate Supercapacitors. *J. Power Sources* **2014**, *248*, 28−36.
(36) Zhou, C.; Zhang, Y.; Li, Y.; Liu, J. Construction of High-Capacitance 3D CoO@Polypyrrole Nanowire Array Electrode for Aqueous Asymmetric Supercapacitor. *Nano Lett.* **2013**, *13*, 2078−2085.
(37) Mai, L.; Aamir, M. K.; Tian, X.; Kalele, M. H.; Zhao, Y.; Lin, X.; Xu, X. Synergistic Interaction between Redox-Active Electrolyte and Binder-Free Functionalized Carbon for Ultrahigh Supercapacitor Performance. *Nat. Commun.* **2013**, *4*, 2041−1723.
(38) Chen, G. Understanding Supercapacitors Based on Nano-Hybrid Materials with Interfacial Conjugation. *Prog. Nat. Sci. Mater. Int.* **2013**, *23*, 245−255.
(39) Meng, C.; Liu, C.; Chen, L.; Hu, C.; Fan, S. Highly Flexible and All-Solid-State Paperlike Polymer Supercapacitors. *Nano Lett.* **2010**, *10*, 4025−4031.